

## Connecting Structural Heterogeneity to Properties of Disordered Materials

Soohyun Im<sup>1</sup>, Gabriel Calderon Ortiz<sup>1</sup>, Mehrdad Abbasi Gharacheh<sup>1</sup>, Robert Williams<sup>2</sup> and Jinwoo Hwang<sup>1</sup>

<sup>1</sup>The Ohio State University, Columbus, Ohio, United States, <sup>2</sup>The Ohio State University, Hilliard, Ohio, United States

Disordered materials are ubiquitous in nature, and many of them, including amorphous and glassy materials, already play a vital role in various applications. Understanding structure-property relationships in disordered materials is, however, challenging due to their complex atomic structure. Despite the absence of long-range atomic arrangement in their structure, it has been known that the atomic ordering at the medium range, which constitutes structural heterogeneity at the nanometer scale, can dictate the important properties of disordered materials. Detailed investigation of MRO is therefore imperative, but difficult because conventional characterization methods, such as using high-resolution imaging or diffraction techniques, are typically not sensitive to the MRO structure.

We show our novel method of determining the detailed structural parameters of MRO and nanoscale heterogeneity in disordered materials using 4-dimensional scanning transmission electron microscopy (4D-STEM) enabled by the new-generation high dynamic range pixelated STEM detectors. Our analysis is based on the reconstruction of the dark-field images of MRO domains using the 4D stack of nanodiffraction patterns acquired continuously over the specimen area (Fig. 1). The 4D-data contains the subtle diffraction signals from MRO that are resolved at the sub-nanometer scale in the real space ( $x, y$ ) as well as the in the reciprocal space ( $k_x, k_y$ ) with the resolution of at least  $0.1 \text{ nm}^{-1}$ . This provides highly rich information about the type, size, distribution, and volume fraction of MRO domains within the disordered structure [1, 2], far beyond the limits of any prior works based on conventional detectors (Fig. 2). High dynamic range of the detector (Electron Microscopy Pixel Array Detector, or EMPAD [3]) also allows for the preservation of the zero beam intensities without saturation, which is essential for the quantitative estimation of important experimental parameters, such as the precise thickness of the TEM specimen.

Our quantitative 4D-STEM analysis establishes important structure-property relationships in several novel disordered systems, including: (1) nanoscale structural heterogeneity in metallic glasses and its impact to their mechanical properties and glass forming ability, (2) MRO in amorphous semiconductors (e.g. a- $\text{B}_x\text{C}_x\text{H}$ , a- $\text{SiN}_x\text{H}$ ) and its connection to the electronic and thermal properties, (iii) nanoscale intermediate phases in amorphous oxides (e.g.  $\text{TiO}_2$ ) and their properties, and (iv) molecular ordering in semiconducting polymers and its influence to the electronic and photovoltaic properties of organic thin films. We acknowledge support from the National Science Foundation under DMR-1709290 and DMREF-1729227, and the Department of Energy under DE-SC0020283.

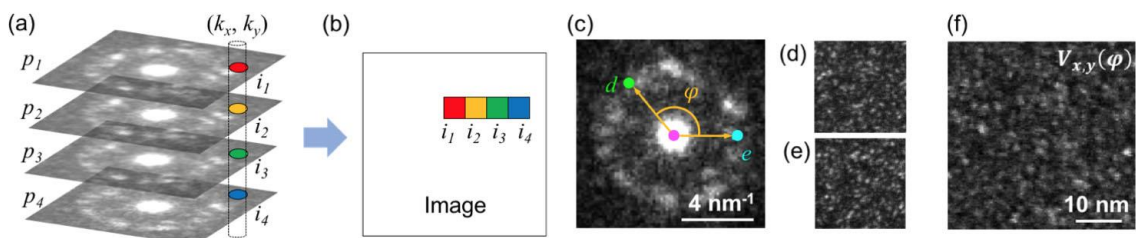


**Figure 1.** (a and b) A schematic showing 4-D STEM of Zr<sub>55</sub>Co<sub>25</sub>Al<sub>5</sub> MG using 1 nm probe. Any pixel in k-space can be selected to form the DF image in real space. DF images shown in (d) and (e) are formed using the k-space positions d and e shown in (c), respectively. (f)  $V_{x,y}(\phi)$  image showing MRO speckles [1].

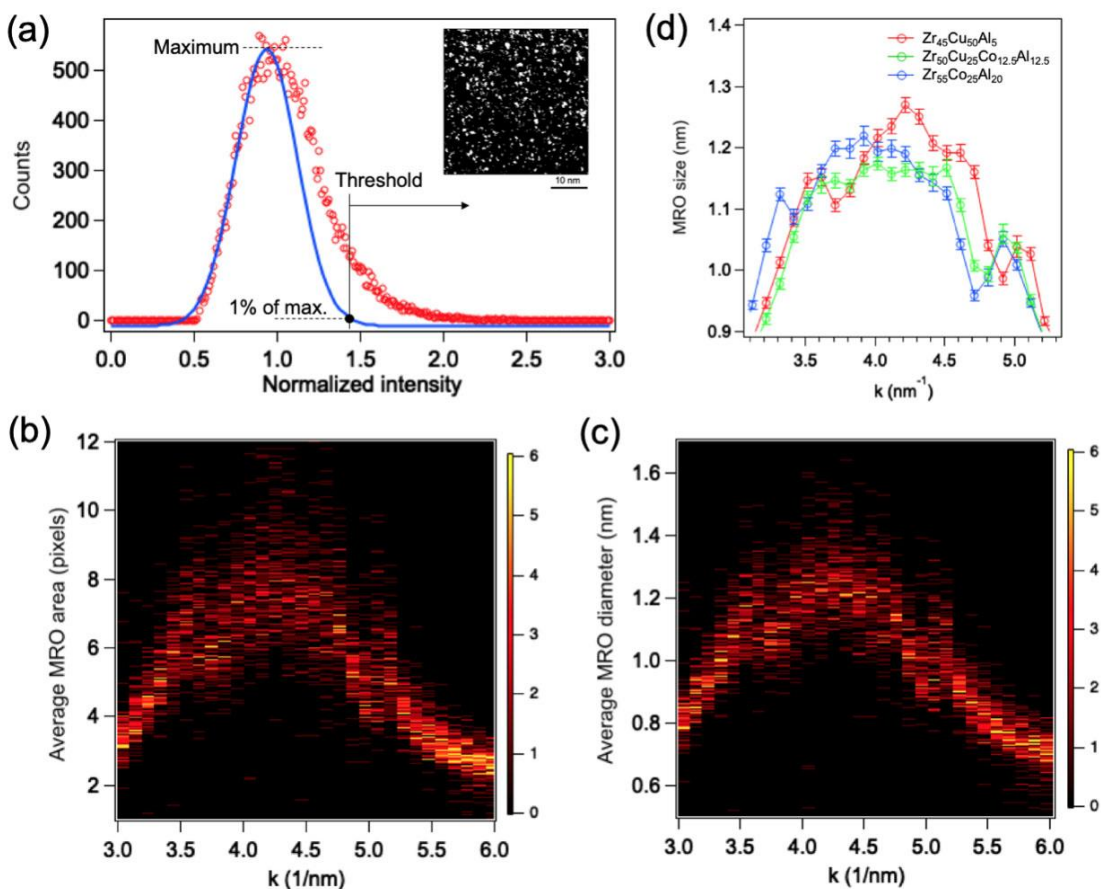


**Figure 2.** (a) A histogram of the normalized pixel intensities within a reconstructed dark field image. The threshold value for the MRO determination was set based on the location of the 1% of the maximum of the Gaussian fit function. The inset shows an example of the threshold masking over the image. (b) 2D-histogram as a function of the average MRO area (in pixels) and k for Zr<sub>45</sub>Cu<sub>50</sub>Al<sub>5</sub>. (c) 2D-histogram as a function of the average MRO size (in nm) and k, made from (b) with the spherical MRO assumption. (d) MRO size vs. k for 3 MG compositions, made using the weighted averaging of the MRO size histogram such as the one shown in (c) [2].

## References

1. Soohyun Im, Zhen Chen, Jared M. Johnson, Pengyang Zhao, Geun Hee Yoo, Eun Soo Park, Yunzhi Wang, David A. Muller, and Jinwoo Hwang, Ultramicroscopy 195, 189 (2018).

2. Soohyun Im, Pengyang Zhao, Geun Hee Yoo, Zhen Chen, Gabriel Calderon, Mehrdad Abbasi Gharacheh, Olivia Licata, Baishakhi Mazumder, David A. Muller, Eun Soo Park, Yunzhi Wang, and Jinwoo Hwang, *Physical Review Letters* (in review).

3. W. Tate, P. Purohit, D. Chamberlain, K. X. Nguyen, R. Hovden, C. S. Chang, P. Deb, E. Turgut, J. T. Heron, D. G. Schlom, D. C. Ralph, G. D. Fuchs, K. S. Shanks, H. T. Philipp, D. A. Muller, and S. M. Gruner, *Microsc. Microanal.* 22, 237 (2016).